JOURNAL OF NATURAL PRODUCTS

Article

pubs.acs.org/jnp

Chaunopyran A: Co-Cultivation of Marine Mollusk-Derived Fungi Activates a Rare Class of 2-Alkenyl-Tetrahydropyran

Zhuo Shang, Angela A. Salim, and Robert J. Capon*

Division of Chemistry and Structural Biology, Institute for Molecular Bioscience, The University of Queensland, St Lucia, QLD 4072, Australia

Supporting Information

ABSTRACT: Co-cultivation of *Chaunopycnis* sp. (CMB-MF028) and *Trichoderma hamatum* (CMB-MF030), fungal strains co-isolated from the inner tissue of an intertidal rock platform mollusc (*Siphonaria* sp), resulted in transcriptional activation of a rare class of 2-alkenyl-tetrahydropyran, chaunopyran A (**7**), and biotransformation and deactivation of the antifungal pyridoxatin (**1**), to methyl-pyridoxatin (**8**). This study illustrates the complexity of offensive and counter-offensive molecular defenses encountered during fungal co-cultivation, and the opportunities for activating new, otherwise transcriptionally silent secondary metabolites.

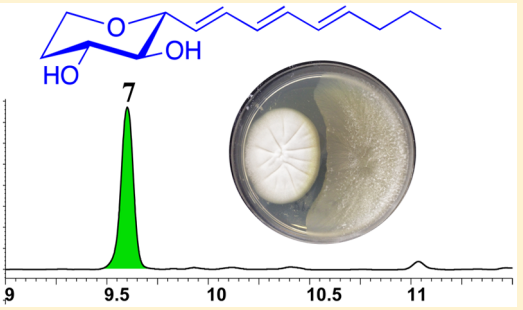

The search for bioactive microbial secondary metabolites has inspired basic and applied science since early in the last century. Notwithstanding a history replete with remarkable successes, traditional biodiscovery is increasingly constrained by excessive rediscovery of known metabolites. That the latter is indicative of technical challenges rather than a depleted resource is evidenced by modern microbial genomics, which has catalogued many thousands of biosynthetic gene clusters (BGCs) encoding an array of unexplored secondary metabolites. That this biosynthetic potential has eluded past efforts at exploration is for the most part explained by the observation that many are transcriptionally silent under standard culture conditions, rendering their gene products (i.e., secondary metabolites) inaccessible. To overcome this impasse requires new cultivation strategies capable of routine and cost-effective activation of silent BGCs. One promising line of inquiry builds on the ecology-inspired hypothesis that silent BGCs are transcriptionally regulated by environmental stimuli, in particular, chemical cues released by other microbes. For example, a chemical cue released by one microbe may elicit an "on-demand" activation of one or more silent BGCs in an opposing strain, leading to the production of defensive secondary metabolite(s). Indeed, these activated defensive metabolites can themselves be chemical cues that trigger a retaliatory transcriptional activation. Inspired by recent successes in co-cultivation-mediated microbial biodiscovery,[1−5] we set out to investigate the possible benefits and practicalities of this approach.

In an earlier report we described the polyketide pyridinones **1**−**2** and tetramic acids **3**−**6** from a *Chaunopycnis* sp. (CMB-MF028) isolated from the inner tissue of a pulmonate false limpet *Siphonaria* sp, collected from intertidal rock platforms near Brisbane, Australia (Figure 1).[6] Based on growing interest in co-cultivation as a method for accessing new metabolites, we

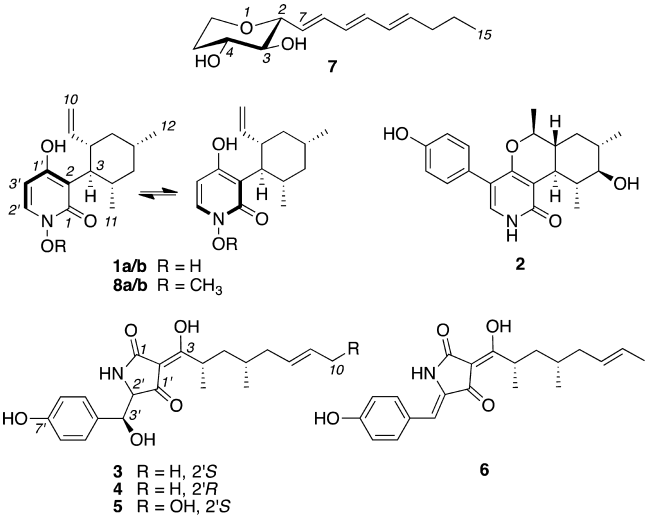

Figure 1. CMB-MF028 metabolites **1a**/**b** and **2**−**6**, and CMB-MF030 co-cultivation products **7** and **8a**/**b**.

speculated that the CMB-MF028 genome may encode silent BGCs under the regulatory control of chemical cues produced by co-isolated fungi. To test this hypothesis, extracts prepared from 30 day ISP2 agar plate co-cultivations of CMB-MF028 with each of five co-isolated fungal strains were subjected to HPLC-DAD-MS analysis (Figure S1). Significantly, only co-cultivation with *Trichoderma hamatum* (CMB-MF030) co-incided with activation of new chemistry (i.e., **7** and **8a**/**b**) (Figure 2). Figure 2A reveals a co-cultivation agar plate with separate growth zones for (i) CMB-MF028 and (ii) CMB-

Received: February 17, 2017

DOI: 10.1021/acs.jnatprod.7b00144
J. Nat. Prod. XXXX, XXX, XXX−XXX

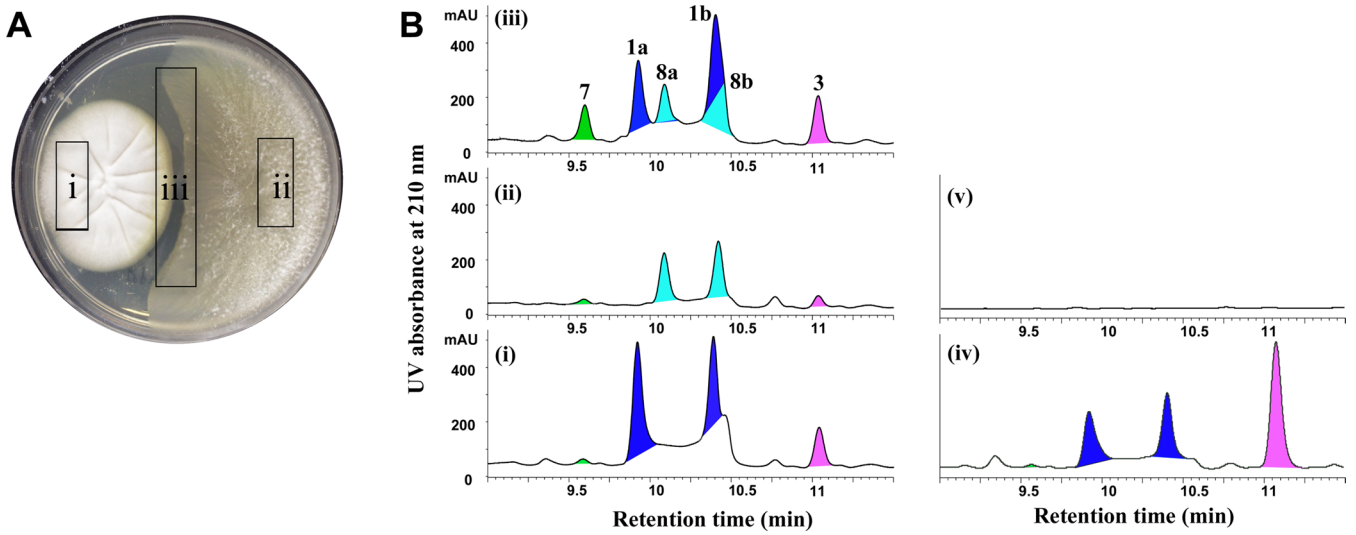

Figure 2. Agar plate co-cultivation of CMB-MF028 and CMB-MF030. (A) Image of the co-culture agar plate, and (B) HPLC-DAD (210 nm) chromatograms of co-culture sampling of (i) CMB-MF028, (ii) CMB-MF030, and (iii) growth inhibitory interface, and of monocultures of (iv) CMB-MF028 and (v) CMB-MF030.

MF030, and (iii) a growth inhibitory interface. Figure 2B features windows (R_t 9−11.5 min) from analytical HPLC-DAD (210 nm) chromatograms of analytes prepared from co-cultivation (i−iii) and monocultures (iv−v) of CMB-MF028 and CMB-MF030. In these analyses the CMB-MF030 monoculture (v) reveals no secondary metabolites, whereas the CMB-MF028 monoculture (iv) reveals the known metabolites **1a**/**b** (equilibrating atropisomers) and **3**. By contrast, in the co-cultivation study, (i) exhibits a chromatogram featuring **1a**/**b** and **3** at levels comparable to that of the CMB-MF028 monoculture (iv); (ii) exhibits low levels of **3**, and the new compounds **8a**/**b** and **7**; and (iii) reveals **1a**/**b**, **3**, **8a**/**b** and 7. UPLC-DAD (254 nm) and HPLC-ESIMS with single ion extraction monitoring analysis could not detect **8a**/**b**, and could only detect extremely low levels of **7** in CMB-MF028 monoculture, a situation that was not changed by altering cultivation conditions or media (Figure S2). Significantly, multiple replicate ISP2 agar plate and ISP2 broth co-cultivations of CMB-MF028 and CMB-MF030 consistently produced **7** and **8a**/**b** in isolable yields (Figure S3).

A time course investigation of ISP2 broth co-cultivations revealed production of **7** and **8a**/**b** at day 1, peaking on day 5, with sustained levels of production across all 8 days of the study (Figures S4). CMB-MF028 was also incubated in the presence of sterile dead mycelia, mycelia acetone extract, and EtOAc and butanol extracts of ISP-2 broth cultivations of CMB-MF030, as well as an EtOAc extract of a co-culture of CMB-MF028 with CMB-MF030; however, none of these conditions increased production of **7** or **8a**/**b** (Figure S5). To investigate this phenomenon further, an EtOAc extract obtained from a scaled up broth co-cultivation (3 L) of CMB-MF028 and CMB-MF030 was subjected to solvent trituration, followed by normal and reversed-phase chromatography to yield **7** and **8a**/**b**.

HRESI(+)MS analysis of **7** returned a sodium adduct ion indicative of a molecular formula ($C_{14}H_{22}O_3$, Δmmu + 0.7) requiring four double bond equivalents (DBE). Analysis of the 1D NMR (DMSO-d_6) data for **7** (Table 1) revealed resonances attributed to a 3,4-dihydroxytetrahydropyran (C-2 to C-6) bearing a C-2 *n*-1,3,5-nonatrienyl side chain (C-7 to C-15), accounting for all four DBE. Diagnostic 2D NMR (DMSO-d_6)

Table 1. ^{1}H (600 MHz) and ^{13}C (150 MHz) NMR Data for Chaunopyran A (7) in DMSO-d_6

position	δ_C, type	δ_H, mult. (*J* in Hz)	COSY	HMBC
2	79.8, CH	3.46, dd (9.0, 5.6)	3, 7	3, 4, 7, 8
3	75.9, CH	2.81, ddd (9.0, 9.0, 5.4)	2, 4, 3-OH	2, 4, 7
4	72.1, CH	3.45, overlap	3, 5*β*, 4-OH	–
5*α*	34.2, CH_2	1.77, ddd (12.2, 5.0, 1.5)	5*β*, 6*β*	3, 4
5*β*		1.42, m	4, 5*α*, 6*α*, 6*β*	4, 6
6*α*	64.9, CH_2	3.79, ddd (11.6, 5.0, 1.5)	5*β*, 6*β*	2, 4
6*β*		3.45, overlap	5*α*, 5*β*, 6*α*	2, 4
7	131.7, CH	5.77, dd (15.4, 5.6)	2, 8	2, 8, 9
8	130.6, CH	6.21, dd (15.4, 10.6)	7, 9	2, 10
9	130.5, CH	6.14, dd (15.1, 10.6)	8, 10	7, 8, 10, 11
10	132.5, CH	6.18, overlap	9, 11	8, 12
11	130.6, CH	6.08, dd (15.1, 10.3)	10, 12	9, 13
12	134.7, CH	5.71, dt (15.1, 7.0)	11, 13	10, 11, 13, 14
13	34.3, CH_2	2.05, dt (7.0, 7.0)	12, 14	11, 12, 14, 15
14	22.0, CH_2	1.37, tq (7.0, 7.3)	13, 15	12, 13, 15
15	13.6, CH_3	0.87, t (7.3)	14	13, 14
3-OH	–	4.94, d (5.4)	3	2, 3, 4
4-OH	–	4.82, d (4.6)	4	3, 4, 5

HMBC and COSY correlations (Figure 3) supported the assigned planar structure, while the magnitudes of $J_{7,8}$ (15.4 Hz), $J_{9,10}$ (15.1 Hz), and $J_{11,12}$ (15.1 Hz) confirmed an all-*E* configuration about the triene moiety. Axial configurations for H-2, H-3, and H-4 were evident from $J_{2,3}$ (9.0 Hz) and $J_{3,4}$ (9.0 Hz), and were confirmed by ROESY correlations between H-3 and 4-OH, and H-2 and 3-OH (Figure 3). Thus, the structure and relative configuration for chaunopyran A (**7**) were assigned as indicated.

To support the proposed structure for **7**, and to address the issue of absolute configuration, the model tetrahydropyran **7c** was synthesized using the methodology outlined in Scheme 1. Adapting a published procedure,[7] a sample of L-rhamnose was

DOI: 10.1021/acs.jnatprod.7b00144
J. Nat. Prod. XXXX, XXX, XXX−XXX

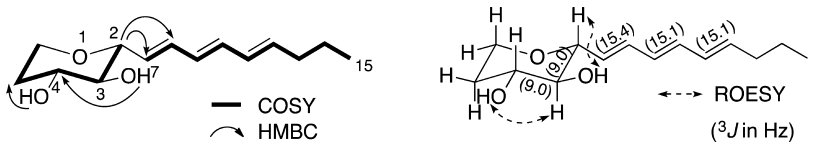

Figure 3. Diagnostic NMR (DMSO-d_6) data and correlations for chaunopyran A (**7**) (* Values in parentheses are ^3J coupling constants).

Scheme 1. Synthesis of Model Tetrahydropyran 7c (i) Ac_2O, HBr/AcOH, Zn/$CuSO_4$ (71%); (ii) H_2, Pd/C, (92%); (iii) NH_4OH, MeOH, (21%)

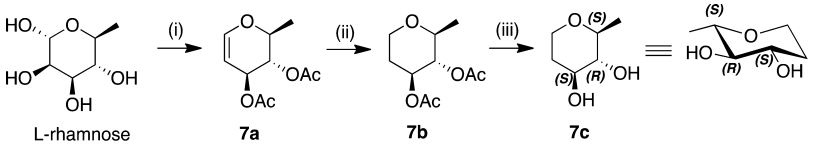

Table 2. ^1H (600 MHz) and ^{13}C (150 MHz) NMR Data for Methyl-Pyridoxatin (8a/b) in DMSO-d_6

	8 (major atropisomer)		**8** (minor atropisomer)	
position	δ_C, type	δ_H[a] mult. (*J* in Hz)	δ_C, type	δ_H,[a] mult. (*J* in Hz)
1	157.5, C	–	159.8, C	–
2	113.2, C	–	113.7, C	–
3	45.8, CH	2.33, dd (10.5, 10.5)	45.7, CH	2.57, dd (11.0, 11.0)
4	41.7, CH	2.99, m	42.8, CH	2.77, m
5a	41.7, CH_2	1.66, m[a]	42.0, CH_2	1.68, m[a]
5b		0.82, m[b]		0.84, m[b]
6	31.4, CH	1.53, m[c]	31.5, CH	1.53, m[c]
7a	44.2, CH_2	1.68, m[d]	44.4, CH_2	1.67, m[d]
7b		0.66, m[e]		0.68, m[e]
8	31.4, CH	2.29, m	32.4, CH	2.13, m
9	143.6, CH	5.49, m[f]	143.4, CH	5.46, m[f]
10a	112.3, CH_2	4.73, ddd (17.2, 2.4, 0.8)[g]	112.4, CH_2	4.74, d (17.2, 2.4, 0.8)[g]
10b		4.62, dd (10.3, 2.4)[h]		4.63, dd (10.3, 2.4)[h]
11	20.6, CH_3	0.63, d (6.6)[i]	20.4, CH_3	0.64, d (6.6)[i]
12	22.8, CH_3	0.89, d (6.6)[j]	22.7, CH_3	0.88, d (6.6)[j]
1′	162.4, C	–	161.4, C	–
2′	133.0, CH	7.58, d (7.8)	132.7, CH	7.55, d (7.8)
3′	97.9, CH	5.83, d (7.8)	98.7, CH	5.80, d (7.8)
N-OCH_3	63.9, CH_3	3.82, s	63.8, CH_3	3.81, s

[a]Resonances with the same superscript letter (a-j) across atropisomers are overlapping.

treated with Ac_2O and catalytic HBr/acetic acid to effect peracetylation, with further addition of HBr/AcOH generating the intermediate anomeric bromide, which on workup in Zn/$CuSO_4$ returned the acetylated glycal **7a**. Subsequent hydrogenation and deacetylation yielded **7b** and **7c**, respectively. The 1D NMR (DMSO-d_6) data for **7c** compared very well with the natural product **7** (Figures S16 and S17), confirming the proposed structure, including relative configuration. Notwithstanding different C-2 side chains, as the $[\alpha]_D$ for **7** (−25, *c* 0.05, MeOH) was opposite in sign to **7c** (+11, *c* 0.15, MeOH), we tentatively propose a 2*R*,3*S*,4*R* absolute configuration for chaunopyran A (**7**) (Figure 1).

Chaunopyran A (**7**) belongs to a rare class of fungal 2-alkenyl-tetrahydropyran, selected examples of which (glycinyl esters) are potent inhibitors of the cytochrome P450 lanosterol C-14 demethylase, and as such exhibit broad-spectrum antifungal activity. The first members of this structure class, reported in 1991 by Merck, Sharpe, and Dohme researchers from *Penicillium restrictum*, were the antifungal glycinyl esters restricticin and *N*,*N*-dimethylrestricticin, and the alcohol restrictinol.[8] In 1992, Roche researchers reported five new congeners (Ro 09−1543, Ro 09−1545, Ro 09−1547, Ro 09−1549, and Ro 09−1544) from *Penicillium* sp. NR6564 and *Aspergillus sclerotiorum* Huber,[9] while Bristol-Myers Squibb researchers reported the glycinyl esters lanomycin and glucolanomycin, and the alcohol lanomycinol from *Pycnidiophora dispersa*.[10] Our discovery of **7** represents the first natural product addition to this structure class in over 30 years. Consistent with established structure activity relationship studies, as **7** did not possess a glycinyl ester moiety it did not exhibit fungicidal or fungistatic activity (against either our assay strain *Candida albicans* (ATCC 90028), or the co-cultivation strain *Trichoderma hamatum* (CMB-MF030)). As co-culture activation of **7** would seem to suggest a defensive response, we were initially perplexed to discover that **7** lacked antifungal activity. Based on prior literature, glycinyl ester analogues of **7** could be expected to have exceptionally potent antifungal properties, and as such may only be produced under co-cultivation conditions at very low concentrations. Unfortunately, all efforts to detect putative glycinyl ester of **7** proved unsuccessful. At this point it is worth noting that, despite a good DAD response, **7** is only weakly responsive to ESIMS analysis. The failure to detect low levels of putative glycinyl

DOI: 10.1021/acs.jnatprod.7b00144
J. Nat. Prod. XXXX, XXX, XXX−XXX

esters may be attributed to their instability during MS ionization.

HRESI(+)MS analysis of **8a/b** returned a sodium adduct ion indicative of a molecular formula ($C_{16}H_{23}NO_3$, Δmmu −0.5) suggestive of a methylated analogue of pyridoxatin (**1a/b**). Comparison of 1D and 2D NMR (DMSO-d_6) data for **8a/b** (Table 2 and Figure 4) with **1a/b** confirmed this hypothesis,

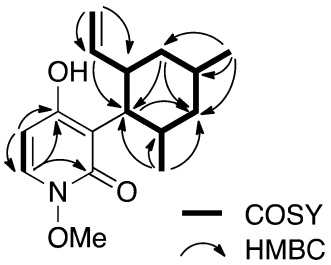

Figure 4. Diagnostic 2D NMR (DMSO-d_6) correlations for methyl-pyridoxatin (**8a/b**).

with the only significant difference being the appearance of resonances for an *N*-OCH_3 moiety (major atropisomer δ_H 3.82; δ_C 63.9; minor atropisomer δ_H 3.81; δ_C 63.8)—as previously documented for **1a/b**, the NMR and HPLC data for **8a/b** revealed major and minor atropisomers (5:3).

Importantly, whereas **1a/b** is a potent siderophore (logK_{app} 34 binding affinity for Fe(III))[6] and is known to exhibit antifungal properties dependent on retaining an unmodified *N*-OH moiety,[11] the *N*-OMe analogue **8a/b** in our hands exhibits no Fe(III) binding affinity, nor is it cytotoxic to mammalian or fungal cells. As **1a/b** is constitutively produced by CMB-MF028,[6] we speculate that under co-cultivation condition CMB-MF030 counters this antifungal agent by biotransforming **1a/b** to **8a/b**. Supportive of this hypothesis, CMB-MF030 cultures treated with an extract of CMB-MF028 rich in **1a/b** effect a quantitative biotransformation of **1a/b** to **8a/b** (Figure 5). Given its relationship to **1a/b**, we attribute a 3*R*,4*S*,6*R*,8*S* absolute configuration to methyl-pyridoxatin (**8a/b**) (Figure 1).

In summary, our observations document complementary chemical-ecology responses encountered during co-cultivation of CMB-MF028 and CMB-MF030 (Figure 2). During co-cultivation, CMB-MF028 deploys a constitutively produced antifungal agent **1a/b** that we propose has the potential to inhibit the growth of CMB-MF030. Confronted by this challenge, CMB-MF030 biotransforms and deactivates **1a/b** to the nonantifungal **8a/b**. As CMB-MF028 continues to produce **1a/b**, and CMB-MF030 continues to biotransform **1a/b** to **8a/b**, the relative kinetics of these processes determines the equilibrium for this encounter—on an agar plate, co-cultivation is evidenced by a growth inhibition interface between these cultures (Figure 2). We speculate that, in an effort to alter the balance of the battle in its favor, and in response to an as yet unknown co-cultivation cue, CMB-MF028 activates a silent PKS to produce chaunopyran A (**7**). Chaunopyran A (**7**) is the first new example of a rare class of fungal 2-alkenyl-tetrahydropyrans to be reported in over 30 years. Prior studies on the structure class determined that glycinyl esters were exceptionally potent antifungals, whereas simple alcohols such as **7** were not antifungal. Whether CMB-MF028 is stimulated by co-culture with CMB-MF030 to produce glycinyl esters of **7** at levels below detection, or whether the BGC is corrupted and lacks the necessary NRPS module for incorporating the glycinyl residue, remains an intriguing, but unresolved question.

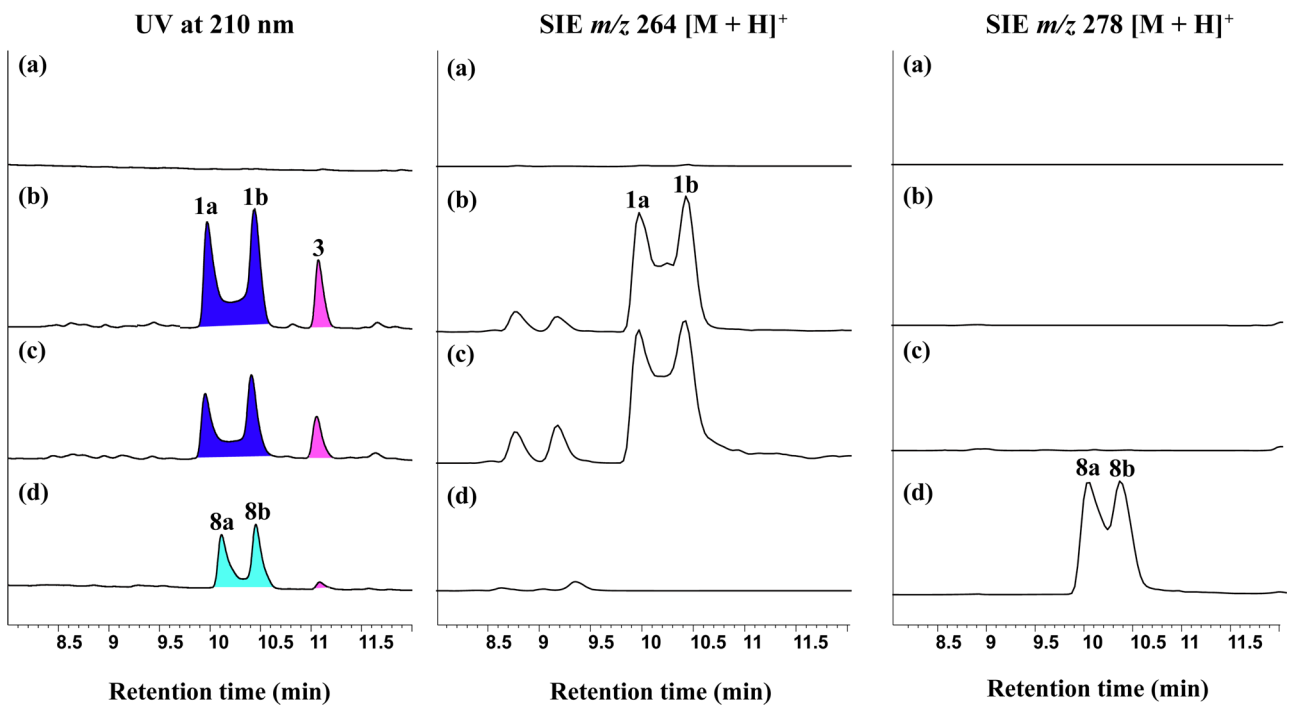

Figure 5. HPLC-DAD (210 nm) chromatograms of CMB-MF030 biotransformation of **1a/b** to **8a/b** and single ion extraction (SIE) with *m/z* 264 and *m/z* 278. (a) Monoculture of CMB-MF030; (b) monoculture of CMB-MF028; CMB-MF030 cultivated in the presence of EtOAc extract of CMB-MF028 on (c) day 0 and (d) day 7. Peaks for metabolites are annotated and highlighted.

DOI: 10.1021/acs.jnatprod.7b00144
J. Nat. Prod. XXXX, XXX, XXX−XXX

EXPERIMENTAL SECTION

General Experimental Procedures. Specific optical rotations ($[\alpha]_D$) were measured on a JASCO P-1010 polarimeter in a 100 × 2 mm cell at room temperature. UV−visible spectra were obtained on a Varian Cary 50 UV−visible spectrophotometer with 1 cm quartz cells. Nuclear magnetic resonance (NMR) spectra were acquired on a Bruker Avance 600 MHz spectrometer with either a 5 mm PASEL 1H/D-13C Z-Gradient probe or 5 mm CPTCI 1H/19F-13C/15N/DZ-Gradient cryoprobe, controlled by TopSpin 2.1 software. In all cases spectra were acquired at 25 °C (unless otherwise specified) in solvents as specified in the text, with referencing to residual ^{1}H or ^{13}C signals in the deuterated solvents. Electrospray ionization mass spectrometry (ESIMS) experiments were carried out on an Agilent 1100 series LC/MSD (quadrupole) instrument in both positive and negative modes. High-resolution ESIMS spectra were obtained on a Bruker micrOTOF mass spectrometer by direct injection in MeCN at 3 μL/min using sodium formate clusters as an internal calibrant. High-performance liquid chromatography-diode array-mass spectrometry (HPLC-DAD-MS) data were acquired on an Agilent 1100 series separation module equipped with an Agilent 1100 series HPLC/MSD mass detector and diode array multiple wavelength detector. Semipreparative and preparative HPLCs were performed using Agilent 1100 series HPLC instruments with corresponding detectors, fraction collectors, and software inclusively. Ultrahigh-performance liquid chromatograph-diode array (UPLC-DAD) data were obtained on an Agilent 1290 infinity UPLC system.

Fungal Collection, Isolation, and Taxonomy. Both of the fungi *Chaunopycnis* sp. (CMB-MF028) and *Trichoderma hamatum* (CMB-MF030) were isolated in 2012 from the inner tissue of a marine pulmonate false limpet *Siphonaria* sp. collected at the rocky intertidal zone of Moora Park, Shorncliffe, Queensland. The fresh *Siphonaria* sample was transported in a sterile tube (50 mL) on ice to the laboratory, where it was rinsed in sterile natural seawater for 1 min and subjected to surface sterilization in 70% EtOH (*v*/*v*) for 30 s after which it was washed with sterile natural seawater to remove traces of EtOH. Subsequently, the sample was dissected under aseptic conditions and the inner tissue placed on PYG agar plates (comprising 2% glucose, 1% peptone, 0.5% yeast extract, 0.02% chloramphenicol, 1.7% sea salt, and 1.5% agar). The plates were sealed and incubated at 26.5 °C for 3−4 weeks. Pure cultures of fungi CMB-MF028 and CMB-MF030 were obtained by single-colony serial transfer on agar plates and then cryopreserved at −80 °C in 15% aqueous glycerol. Fungus CMB-MF028 formed circular white colonies with fan-shaped wrinkles and no spores on peptone yeast glucose (PYG) agar and ISP-2 agar. Fungus CMB-MF030 grew quickly with white floccus aerial hyphae and yellow-green spores after 10 days cultivation on PYG agar. The BLAST search showed the amplified ITS sequence for CMB-MF028 (GenBank accession no. KP881722) has 98% homology with other members of the genus *Chaunopycnis* sp., and ITS sequence for CMB-MF030 (GenBank KU593648) has 100% homology with other members of the species *T. hamatum*.

Analytical Cultivation and Chemical Profiling of Co-Culture in ISP-2 Broth. The co-culture of CMB-MF028 and CMB-MF030, inoculated from their respective seed culture (2 mL for each culture), was cultivated at 180 rpm for 5 days in a Schott flask (250 mL) containing ISP-2 broth (0.4% glucose, 0.4% yeast extract, and 1% malt extract in 50 mL distilled H_2O). After cultivation, the broth was extracted with EtOAc (50 mL) and the organic phase concentrated in vacuo to yield an organic extract (7.6 mg). A solution of the extract prepared in MeOH (5 mg/mL) was subjected to HPLC-DAD-MS analysis (Zorbax SB-C_8 column, 150 × 4.6 mm, 5 μm, 1 mL/min gradient elution from 90% H_2O/MeCN to 100% MeCN over 15 min with isocratic 0.05% formic acid modifier). The EtOAc extract for the monoculture control of CMB-MF028 and CMB-MF030 was also analyzed using the same HPLC method.

Analytical Cultivation and Chemical Profiling of Co-Culture on ISP-2 Agar. Fungus CMB-MF028 was inoculated with a single colony on the left side (2 cm from the edge) of an ISP-2 agar plate. After 5 days, fungus CMB-MF030 was inoculated on the right side (2 cm to the edge) of the same agar plate, by the same method. The co-culture plate of CMB-MF028 and CMB-MF030 was incubated at 26.5 °C for 5 days, after which it was sliced into three parts, as shown in Figure 2A. Each part was extracted with EtOAc, and concentrated in vacuo to yield extracts which were resuspended in MeOH (5 mg/mL) and analyzed by HPLC-DAD-MS (Zorbax SB-C_8 column, 150 × 4.6 mm, 5 μm, 1 mL/min gradient elution from 90% H_2O/MeCN to 100% MeCN over 15 min with isocratic 0.05% formic acid modifier).

Production, Isolation, and Characterization of 7 and 8a/b. A scaled-up (3 L) ISP-2 broth of co-cultivation of *Chaunopycnis* sp. (CMB-MF028) and *T. hamatum* (CMB-MF030) was incubated at 180 rpm/min at 26.5 °C for 5 days. An EtOAc extract (501.0 mg) was generated and sequentially triturated to afford hexane (0.7 mg), CH_2Cl_2 (202.5 mg), and MeOH (301.0 mg) soluble fractions. HPLC-DAD analysis localized the induced metabolites in the CH_2Cl_2 and MeOH fractions, which were combined and subjected to reversed-phase (C_{18}) SPE and preparative HPLC fractionation (Luna C_{18} column, 250 × 21.2 mm, 10 μm, 20 mL/min gradient elution from 85% to 10% H_2O/MeCN over 20 min) to afford chaunopyran A (**7**) (t_R = 12.7 min; 1.5 mg, 0.3% of EtOAc extract) and the crude methyl-pyridoxatin (**8a/b**) (t_R = 13.4−14.4 min; 6.0 mg) contaminated with a small amount of pyridoxatin (**1a/b**). The latter fraction was further purified by normal phase column chromatography (SiO_2; petroleum ether:acetone 5:1−2:1) to afford pure methyl-pyridoxatin (**8a/b**) (5.5 mg, 1.1% of EtOAc extract).

Chaunopyran A (7). Pale yellow oil; $[\alpha]_D^{22}$ − 25 (*c* 0.05, MeOH); UV−vis (MeOH) λ_{max} (log ε) 260 (3.71), 269 (3.77), 279 (3.69) nm; 1D and 2D NMR (600 MHz, DMSO-d_6) data, Table 1 and Figures S6 and S7; ESI(+)MS *m*/*z* 221 $[M - H_2O + H]^+$, 203 $[M - 2H_2O + H]^+$; HRESIMS *m*/*z* 261.1454 $[M + Na]^+$ (calcd for $C_{14}H_{22}O_3Na$, 261.1461).

Methyl-Pyridoxatin (8a/b). White powder; $[\alpha]_D^{22}$ − 15 (*c* 0.12, MeOH); UV−vis (MeOH) λ_{max} (log ε) 285 (3.84) nm; 1D and 2D NMR (600 MHz, DMSO-d_6) data, Table 2 and Figures S8 and S9; ESI(+)MS *m*/*z* 278 $[M + H]^+$, ESI(−)MS *m*/*z* 276 $[M - H]^-$; HRESIMS *m*/*z* 300.1575 $[M + Na]^+$ (calcd for $C_{16}H_{23}NO_3Na$, 300.1570).

Chemical Synthesis of 7c. L-Rhamnose monohydrate (1.0 g) suspended in Ac_2O (3.5 g, 6.2 mol equiv) was treated at room temperature (rt) with 22% HBr/AcOH (0.1 g). After stirring for 1 h, an additional aliquot of 22% HBr/AcOH (10.5 g, 5.3 mol equiv) was introduced and the mixture stirred overnight, after which anhydrous NaOAc (2.5 g) was added to neutralize the excess HBr, and the resulting solution treated with Zn (10.0 g) and $CuSO_4$ (0.16 g suspended in H_2O (10 mL) and AcOH (5 mL) containing sodium acetate (7.5 g). The resulting mixture was stirred vigorously at rt for 3 h, after which it was partitioned between H_2O (100 mL) and EtOAc (100 mL). The EtOAc solubles were washed successively with H_2O (100 mL), saturated aqueous $NaHCO_3$ (100 mL), and saturated brine (100 mL), after which they were concentrated in vacuo to yield a colorless oil which was purified by column chromatography (SiO_2; petroleum ether: EtOAc 30:1−15:1) to afford the acetylated glycal **7a** (310.7 mg, 31%). Subsequently, **7a** was dissolved in MeOH (10 mL) and hydrogenated in the presence of Pd/C (31 mg) for 1.5 h to yield **7b** (286.6 mg, 92%) as colorless oil. A sample of **7b** in MeOH (5 mL) was treated with K_2CO_3 (100 mg) and stirred for 15 min to yield, after standard solvent extraction, a colorless oil, which was purified by column chromatography (SiO_2, increasing polarity from CH_2Cl_2:MeOH (40:1) to CH_2Cl_2:MeOH(20:1) to afford **7c** (58.9 mg, 21%).

7a. Colorless oil; ^{1}H NMR ($CDCl_3$) δ_H 4.11 (dq, *J* = 8.3, 6.6 Hz, H-2), 5.03 (dd, *J* = 8.3, 6.2 Hz, H-3), 5.34 (ddd, J = 6.2, 3.0, 1.2 Hz, H-4), 4.78 (dd, *J* = 6.2, 3.0 Hz, H-5), 6.43 (dd, *J* = 6.2, 1.2 Hz, H-6), 1.31 (d, *J* = 6.6 Hz, H-7), 2.09 (s, 3-OAc), 2.04 (s, 4-OAc); ^{13}C NMR ($CDCl_3$) δ_C 72.7 (C-2), 72.0 (C-3), 68.5 (C-4), 99.0 (C-5), 146.2 (C-6), 16.8 (C-7), 21.1 (3−$OCOCH_3$), 21.3 (4−$OCOCH_3$), 170.1 (3-$OCOCH_3$), 170.9 (4-$OCOCH_3$); HRESIMS *m*/*z* 237.0744 $[M + Na]^+$ (calcd for $C_{10}H_{14}O_5Na$, 237.0739).

7b. Colorless oil; ^{1}H NMR ($CDCl_3$) δ_H 3.39 (dq, *J* = 9.4, 6.2 Hz, H-2), 4.72 (dd, *J* = 9.4, 9.4 Hz, H-3), 4.92 (ddd, *J* = 11.5, 9.4, 5.3 Hz, H-4), 2.06 (m, H-5a), 1.78 (tdd, *J* = 12.8, 11.5, 5.1 Hz, H-5b), 3.94 (ddd,

DOI: 10.1021/acs.jnatprod.7b00144
J. Nat. Prod. XXXX, XXX, XXX−XXX

J = 11.9, 5.1, 1.7 Hz, H-6a), 3.47 (ddd, J = 11.9, 11.9, 2.1 Hz, H-6b), 1.18 (d, J = 6.2 Hz, H-7), 2.05 (s, 3-OAc), 2.02 (s, 4-OAc); ^{13}C NMR ($CDCl_3$) δ_C 74.9 (C-2), 74.8 (C-3), 72.6 (C-4), 31.6 (C-5), 65.3 (C-6), 18.1 (C-7), 21.1 (3-OCOCH_3), 21.3 (4-OCOCH_3), 170.4 (3-O$COCH_3$), 170.8 (4-O$COCH_3$); HRESIMS m/z 239.0897 $[M + Na]^+$ (calcd for $C_{10}H_{16}O_5Na$, 239.0895).

7c. Colorless volatile oil; $[\alpha]_D^{22}$ + 11 (c 0.15, MeOH); ^{1}H NMR ($CDCl_3$) δ_H 3.21 (dq, J = 9.1, 6.1 Hz, H-2), 3.08 (dd, J = 8.9, 8.9 Hz, H-3), 3.58 (ddd, J = 11.4, 8.9, 5.1 Hz, H-4), 1.96 (ddt, J = 12.9, 5.1, 1.9 Hz, H-5a), 1.71 (tdd, J = 12.9, 11.4, 5.0 Hz, H-5b), 3.92 (ddd, J = 11.8, 5.0, 1.6 Hz, H-6a), 3.45 (ddd, J = 12.6, 11.8, 2.1 Hz, H-6b), 1.30 (d, J = 6.1 Hz, H-7); ^{13}C NMR ($CDCl_3$) δ_C 76.3 (C-2), 78.5 (C-3), 73.5 (C-4), 34.0 (C-5), 65.8 (C-6), 18.2 (C-7).

Biotransformation of 1a/b to 8a/b by CMB-MF030. The EtOAc extract (50 mg, containing **1a**/**b** as the major component) of 7 days' cultivated fungus *Chaunopycnis* sp. (CMB-MF028) was added to 500 mL ISP-2 broth followed by inoculation of fungus *T. hamatum* (CMB-MF030) seed culture and incubation for 7 days at 180 rpm at 26.5 °C. An aliquot (25 mL) of the 0 day and 7 days' broth was extracted with EtOAc respectively, followed by drying the organic phase in vacuo to yield extracts. The extracts as well as the extracts from 7 days' monoculture of CMB-MF028 and CMB-MF030 under the same cultivation condition were prepared at the concentration of 5 mg/mL and analyzed on HPLC-DAD-MS (Zorbax SB-C_8 column, 150 × 4.6 mm column, 5 μm, 1 mL/min gradient elution from 90% H_2O/MeCN to 100% MeCN over 15 min, with constant 0.05% formic acid modifier). Single ion extraction (SIE) with the protonated molecules m/z 264 $[M + H]^+$ for **1a**/**b** and m/z 278 $[M + H]^+$ for **8a**/**b** was performed on Agilent ChemStation software.

■ ASSOCIATED CONTENT

Supporting Information

The Supporting Information is available free of charge on the ACS Publications website at DOI: 10.1021/acs.jnatprod.7b00144.

General experimental, fungal taxonomy, HPLC chromatograms of co-cultivation study, bioassays, and NMR spectra of **7**, **7a**−**7c**, and **8a**/**b** (PDF)

■ AUTHOR INFORMATION

Corresponding Author

*E-mail: r.capon@uq.edu.au.

ORCID

Robert J. Capon: 0000-0002-8341-7754

Notes

The authors declare no competing financial interest.

■ ACKNOWLEDGMENTS

We thank B. P. Espósito (University of São Paulo) for helpful advice on assaying Fe(III) binding affinity and Z. G. Khalil (UQ) for cytotoxicity assay. Z. S. acknowledges the provision of the International Postgraduate Research Scholarships (IPRS) and the Centennial Scholarships by the University of Queensland. This research was funded in part by the Institute for Molecular Bioscience, the University of Queensland and the Australian Research Council (DP120100183).

■ REFERENCES

(1) Pettit, R. K. *Appl. Microbiol. Biotechnol.* **2009**, *83*, 19−25.

(2) Bertrand, S.; Bohni, N.; Schnee, S.; Schumpp, O.; Gindro, K.; Wolfender, J. L. *Biotechnol. Adv.* **2014**, *32*, 1180−1204.

(3) Marmann, A.; Aly, A. H.; Lin, W.; Wang, B.; Proksch, P. *Mar. Drugs* **2014**, *12*, 1043−1065.

(4) Moody, S. C. *Future Microbiol.* **2014**, *9*, 575−578.

(5) Netzker, T.; Fischer, J.; Weber, J.; Mattern, D. J.; König, C. C.; Valiante, V.; Schroeckh, V.; Brakhage, A. A. *Front. Microbiol.* **2015**, *6*, 299.

(6) Shang, Z.; Li, L.; Espósito, B. P.; Salim, A. A.; Khalil, Z. G.; Quezada, M.; Bernhardt, P. V.; Capon, R. J. *Org. Biomol. Chem.* **2015**, *13*, 7795−7802.

(7) Shull, B. K.; Wu, Z.; Koreeda, M. *J. Carbohydr. Chem.* **1996**, *15*, 955−964.

(8) Schwartz, R. E.; Dufresne, C.; Flor, J. E.; Kempf, A. J.; Wilson, K. E.; Lam, T.; Onishi, J.; Milligan, J.; Fromtling, R. A.; Abruzzo, G. K.; Jenkins, R.; Glazomitsky, K.; Bills, G.; Zitano, L.; Mochales Del Val, S.; Omstead, M. N. *J. Antibiot.* **1991**, *44*, 463−471.

(9) Matsukuma, S.; Ohtsuka, T.; Kotaki, H.; Shirai, H.; Sano, T.; Watanabe, K.; Nakayama, N.; Itezono, Y.; Fujiu, M.; Shimma, N.; Yokose, K.; Okuda, T. *J. Antibiot.* **1992**, *45*, 151−159.

(10) O'Sullivan, J.; Phillipson, D. W.; Kirsch, D. R.; Fisher, S. M.; Lai, M. H.; Trejo, W. H. *J. Antibiot.* **1992**, *45*, 306−312.

(11) Chang, W.; Zhang, M.; Li, Y.; Li, X.; Gao, Y.; Xie, Z.; Lou, H. *Biochim. Biophys. Acta, Gen. Subj.* **2015**, *1850*, 1762−1771.

DOI: 10.1021/acs.jnatprod.7b00144
J. Nat. Prod. XXXX, XXX, XXX−XXX